STRONG MICROSTREAMING FROM A PINNED OSCILLATING MEMBRANE AND APPLICATION TO GAS EXCHANGE

Anthony L. Mercader and Sung Kwon Cho* University of Pittsburgh, Pittsburgh, Pennsylvania, USA

ABSTRACT

We present a novel configuration to generate strong acoustic streaming vortices by a pinned oscillating membrane in a microchannel, its characterizations via advanced measurement techniques, and initial studies in application by augmentation of gas exchange across a permeable membrane towards microfluidic artificial lung technology. The configuration is stable over time and does not create any obstruction in flow passages. For an audiblefrequency 20 V_{pp} input to a piezo buzzer, streaming velocity was measured up to 47 mm/s. Mixing from helical flow patterns in the microchannel augments gas transfer rate across the membrane up to 3.4 times compared to no actuation, allowing larger channel dimensions (better facilitation of scale-up manufacturing) and reduced shear (more hemocompatible) in microchannel-based artificial lung systems.

KEYWORDS

Acoustofluidics, Microstreaming, Artificial Lung

INTRODUCTION

Acoustic microstreaming in microfluidic devices is often used as a means to disrupt the typically laminar flows seen at the micro-scale for various purposes such as mixing and propulsion [1-3]. In this phenomenon, an oscillating acoustic input can interact with certain features in a flow field to generate time-averaged flows, typically in the form of vortices. It overcomes the limits of low Reynolds number flows due to generation of high local velocity which allows inertial forces to become significant in relation to viscous forces [4, 5].

Many works studying this phenomenon use ultrasound as the input [6, 7] since the effect can scale with frequency due to higher oscillatory velocity [8]. The work here, however, focuses on audible frequency effects where there exists a more limited number of transduction methods to generate the flows because the acoustic wavelength is much longer than any characteristic dimension in the system, meaning one cannot rely on any mechanism which occurs at the scale of that wavelength. Despite the scaling of the strength of the effect, acoustic streaming at audible

frequency can carry some benefits including being cheaper to generate with commercial actuators without requiring precise design of an interdigitated electrode, for example. Among the methods which still work at audible frequency is bubble microstreaming, where a gas bubble resonates and the streaming flow is driven by oscillation of the liquid gas interface [9]. Though the effect is strong, it suffers critical disadvantages including stability due to growth of dissolution of the bubbles and limited applicability to medical devices where contact of bubbles with blood is highly undesirable. More recently discovered is sharp edge streaming where acoustic velocity oscillations in the presence of a sharp tip generates a pair of counter rotating vortices as fluid particles driven in the direction of that tip are directed away by centrifugal effects due to the sharp radius of curvature [10]. While this phenomenon does not suffer from the stability issue, the strength of the effect can be lower and obstruction in a microchannel is a new disadvantage.

This paper presents a novel configuration to generate acoustic microstreaming flows at audible frequency by a pinned, oscillating membrane. A microchannel is formed with polymethylsiloxane (PDMS) as the bottom wall, which is bonded to a glass substrate so that the channel 'hangs' off exposing the membrane to open air. When an acoustic wave is sent through the rigid glass substrate, it is focused on the glass edge creating strong flexural oscillations and thus strong vortex flow patterns above the membrane (Fig 1 (a)).

The focused application here is the microfluidic artificial lung, a device which seeks to oxygenate and/or decarbonate blood by blood and gas microchannels separated by a gas permeable PDMS membrane [11]. Applying active mixing by microstreaming enables both better gas transfer performance and larger channel sizes, greatly reducing shear and potential clotting response in blood. Using the newly described microstreaming concept, a gas transfer device is designed which shows up to 3.4 times improvement in gas exchange efficiency compared to no acoustic actuation.

EXPERIMENTAL

Fabrication

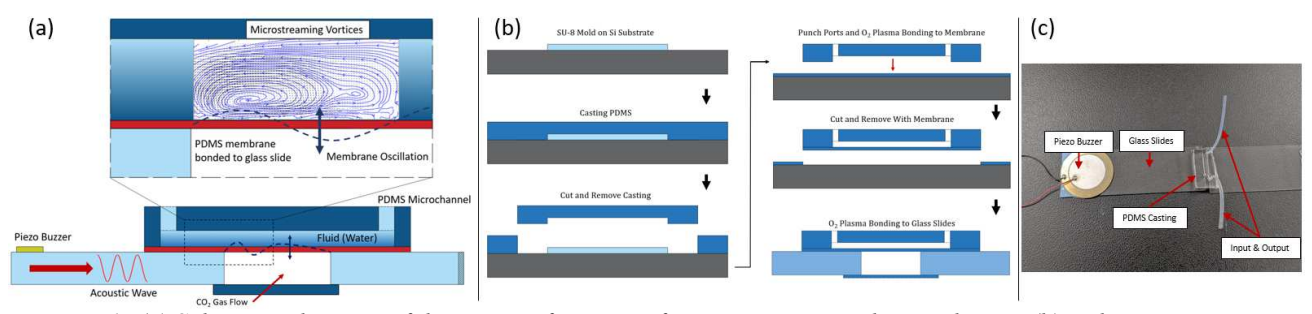


Figure 1: (a) Schematic diagram of the new configuration for microstreaming by membrane; (b) Fabrication process flow; (c) Sample fabrication.

Fabrication details for the base configuration as shown in Fig 1 (b) are as follows. The standard soft lithography process is used to create a mold in the shape of the microchannel. First, a spin coater is used to spread SU-8 2075 negative photoresist in an even layer on top of a silicon wafer up to a maximum of 300 µm depending on spin speed. The resin is cured on a hot plate. The process is repeated in multiple layers for channel heights above 300 μm. The photoresist is exposed to UV light using a mask aligner in an area defined by a photolithography mask in the shape of the top view of the channel. The design used for the initial characterization of the flow to be described used a channel cross section of 600 x 600 µm and length around 1 cm. The exposed photoresist is submerged in SU-8 developer chemical to remove the area of SU-8 which was not exposed to UV light, leaving a negative mold of the channel. PDMS elastomer base and curing agent are mixed in the standard 10:1 ratio, poured over the mold, and cured. The casting is then cut and removed from the mold by hand and the inlet and outlet holes are created by a 1 mm biopsy punch.

The membrane is fabricated by spin coating PDMS in a 20 μ m layer curing as mentioned above. The bottom face of the channel cutout and the membrane are then chemically bonded using a handheld corona air plasma generator. The plasma head is held above the surfaces to be bonded together for 1 minute each, then the channel cutout is pressed onto the membrane surface and left overnight. The membrane with bonded channel cutout is then cut and peeled away from the Si substrate with a razor blade. The bonding process is then repeated as described to bond the underside of the membrane between two glass slides with a desired gap.

23 gauge PTFE tubing is inserted into the inlet and outlet holes and the channel is filled with liquid by a syringe. A piezo buzzer element is attached to one of the glass slides by epoxy to transmit the acoustic waves given a sinusoidal voltage input from a function generator and amplifier. An image of a completed device of this type is shown in Fig 1 (c) The system is viewed with a microscope and high speed camera to confirm the streaming flows. The frequency input is swept to find the frequency which leads to the strongest streaming flow for each sample fabricated, typically between 5 and 7.5 kHz due to sample-to-sample variation.

Laser Doppler Vibrometry (LDV)

In order to characterize its oscillation pattern and investigate the driving mechanism behind the streaming flows, LDV measurement was performed on the section of the membrane exposed to open air. LDV is a measurement technique which shines a laser onto the sample and measures the reflection in such a way that it can characterize the magnitude and phase over a specified frequency spectrum. Because the measurement requires a reflective surface, a slightly different PDMS membrane is fabricated with two layers of spin coating for the same total thickness and a 50 nm layer of Ti in sandwiched in the middle deposited by e-beam evaporation, thin enough to have minimal effect on the oscillation characteristics. The underside of the membrane is aligned with the view of the microscope objective and a grid of measurement points is

specified over the area of interest. The oscillation is measured on the range of 2.5 to 20 V_{pp} at the resonance frequency of 5.5 kHz. Displacement magnitude and phase at each measurement point are exported for later use.

Particle Image Velocimetry (PIV)

Micro PIV (μ PIV) is used to measure the velocity field of the streaming effect. Laser light is guided through a filter cube and microscope objective to excite fluorescent particles seeded in the fluid field. Two images are captured with a specified time delay and correlated by computer software to track the particle motions and calculate a velocity field. In this particular case, the light is guided by a right-angle prism to capture a side view of the streaming, and the time delay was specified at integer multiples of the acoustic period to cancel any phase effects. Measurements were performed on the same input range as with LDV.

Computational Fluid Dynamics (CFD) Simulation

CFD simulation using the CFX solver in ANSYS is performed to confirm the membrane oscillation as the driving mechanism of the streaming flows. Geometry was created to match the dimensions of the fabricated channels. The inlet and outlet were left open, and the top and side walls were rigid, no-slip walls. The membrane oscillation magnitude and phase from LDV measurement were applied as a boundary motion to the bottom wall. The transient simulation is performed with 64 time steps per period of oscillation for a number of periods until the solution between periods does not vary. The streaming flow is visualized by calculating the time average of the velocity field over all the time steps in the final period.

Gas Exchange

For gas exchange, a separate channel geometry was designed so that the glass edge is aligned with the channel length so that the axis of rotation of the vortices is aligned in the same direction and a streamwise flow leads to helical patterns. The new channel width is 1.6 mm and the height varied from $250 \ \mu \text{m}$ to $1 \ \text{mm}$. A PDMS slab is bonded to

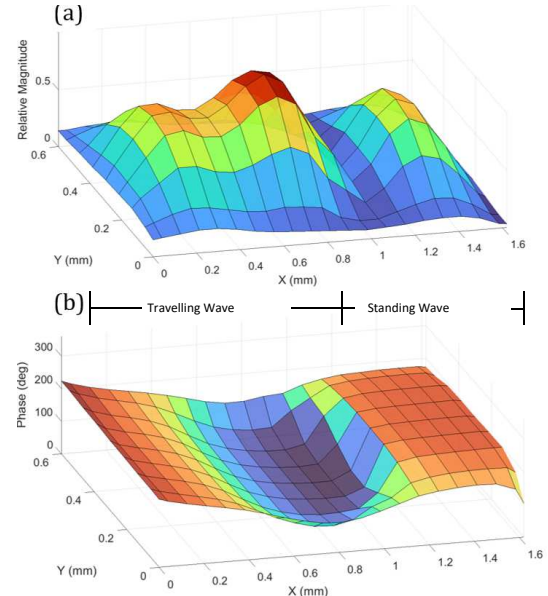


Figure 2: Experimental measurement of membrane oscillation by Laser Doppler Vibrometry (LDV): (a) magnitude and (b) phase.

the underside of the substrate to seal a gas channel. Deionized (DI) water is input by a syringe pump at flow rates of 0.2 and 0.4 mL/min and CO_2 is input by a separate syringe pump to the gas channel at a constant 0.4 mL/min. The pH of the output is measured by a pH meter with a micro pH electrode to characterize the CO_2 transfer into the liquid channel.

RESULTS AND DISCUSSION

Membrane Oscillation

As seen from the magnitude and phase plots in Fig 2, the observed pattern is a superposition of travelling and standing waves starting at the glass edge from which the acoustic waves originate. The travelling wave component dominates near that same edge and gives way to a standing wave dominant portion close to the opposite glass edge, The largest velocity gradient and magnitude appear nearest the primary glass edge, which corresponds to the main vortex and fastest velocity observed in the streaming flow field. On the 2.5 to 20 V_{pp} range of input voltage, the maximum displacement amplitude in the membrane ranged from 2.3 μm to 18.5 μm with approximately linear scaling with voltage.

Velocity Field Measurement

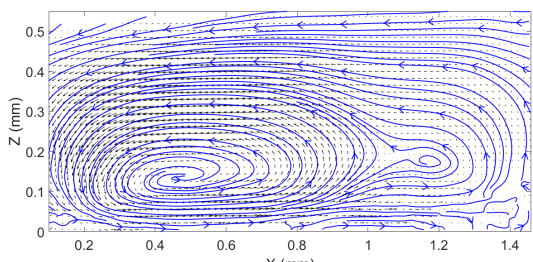


Figure 3: Experimental measurement of velocity fieled and streamline by Particle Image Velocimetry (PIV) (1.5 mm membrane length).

The PIV data give a clear picture of the streaming patterns. For the representative configuration presented in Fig 3, primary vortex with maximum velocity at the bottom is seen corresponding to the leading glass edge and first membrane amplitude peak. A second, corotating vortex is seen, and a third, counterrotating vortex is observed visually outside of the PIV field of view. Maximum velocity ranged from 0.41 mm/s to 47 mm/s on the same input voltage range.

CFD Simulation and Comparison

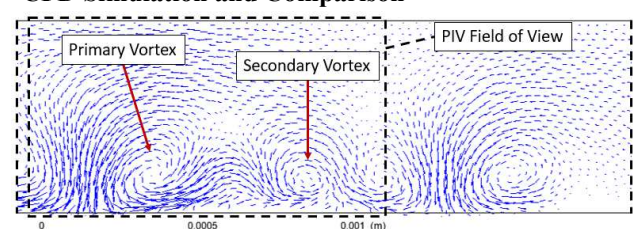


Figure 4: CFD results given membrane oscillation as input.

With the displacement magnitude and phase from the LDV data applied to CFD, the simulation results show good agreement in pattern and magnitude to the PIV results, providing evidence that the mechanical oscillation

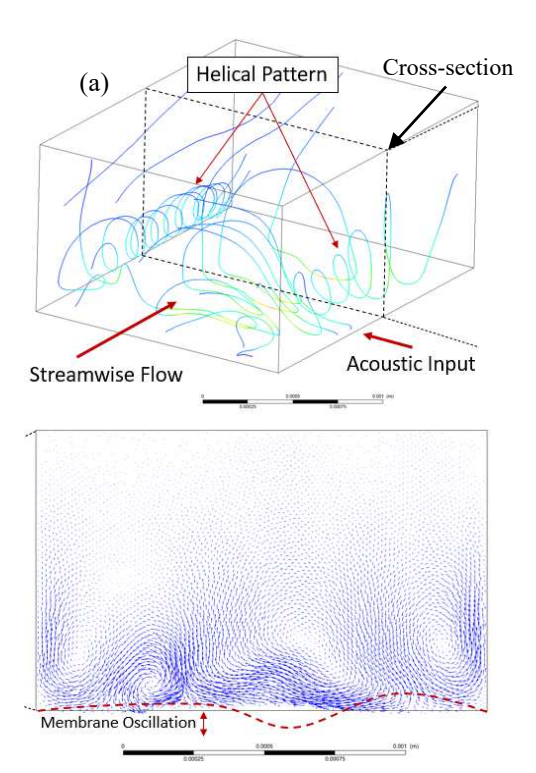


Figure 5: CFD simulation with infused streamwise flow shows (a) representative helical streamlines and (b) cross-sectional velocity field. Note that the membrane oscillating wave is in the cross-channel direction.

of the membrane is the driving mechanism of the acoustic streaming vortices. Especially for the representative 1.5 mm membrane length case, the whole three-vortex system is correctly predicted by simulation, including the fine detail of the very slow corotating vortex within the primary vortex, as seen in Fig 4.

The input amplitude of displacement for the simulation is related to the input voltage in the PIV experiment through the LDV results. In both cases tested, the velocity was predicted well, though slightly higher than experiment by close to 15% at higher input amplitudes. The scaling was approximately quadratic just as in experiment.

A similar simulation was performed on the previously mentioned perpendicular orientation using the centerline LDV magnitude and phase applied as a constant profile along the streamwise direction. The cross-sectional velocity profile appeared similar to the velocity field before, as expected considering the same membrane oscillation profile was used, just turned 90°. Adding channel flow as a constant velocity at the inlet and outlet shows the helical streamlines as desired as shown in Fig 5.

Augmentation of Gas Exchange

The data for each liquid flow rate are presented in Fig 6. Comparing the channel heights, at no actuation, CO₂ transfer through the permeable membrane was greater or equal for the shorter channel at any flow rate. This is in line with expectation due to the fact that the taller channel will tend to be more diffusion limited, although there is the competing effect of lower velocity and therefore larger residence time of the liquid over the membrane at a given flow rate with the taller channel. At any level of actuation applied, the taller channel outperforms the shorter channel,

up to 3.4x compared to no actuation. This is in line with the original goal for the experiment, demonstrating the dual benefit of this method: the gas transfer performance is increased outright and favors a larger channel height which may lead to increased hemocompatibility due to highly reduced shear. Comparing the flow rates, output concentration decreased with increasing flow rate, though the total volume output of liquid at that concentration is increased leading to potentially higher magnitude of gas transfer. Due to these competing effects, the optimal flow rate will likely depend on the needs of the target application.

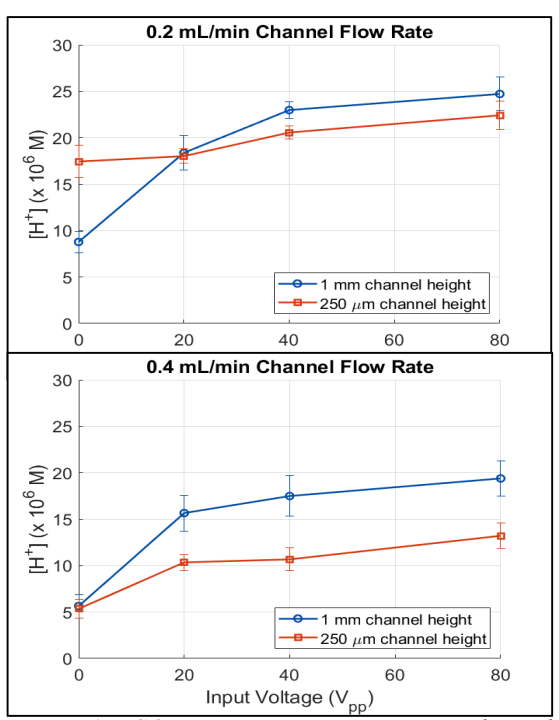


Figure 6: CO₂ concentration in microchannel by measuring pH for probing gas transfer rate at two water flow rates (CO₂ gas flow rate: 0.4 ml/min).

CONCLUSION

A novel configuration to generate audible frequency acoustic streaming flows in a microchannel is presented. A PDMS microchannel with a membrane as the bottom wall is bonded to a glass substrate extending over the edge so that acoustic input sent through the substrate is focused into a flexural oscillation in the membrane, which drives streaming flows in the form of vortices in the channel. The membrane oscillation and streaming flow field were measured by LDV and PIV, respectively, and CFD simulation using the LDV results as a boundary condition shows good agreement, indicating that the membrane oscillation is the driving mechanism and the shorter wavelength of that mechanical vibration compared to the acoustic wavelength allows the phenomenon to operate at audible frequency. Due to the vertical orientation of the mixing and requirement of membrane interface with open air, gas exchange towards microfluidic artificial lung technology is seen as the target application. A gas exchange device was fabricated with a gas channel formed on the underside of the membrane. With DI water input to the liquid side and CO₂ input to the gas side, pH measurement characterizes the magnitude of CO₂ transfer into the liquid side. Results show a taller channel outperforming a shorter channel at any level of actuation tested demonstrating a dual benefit of increased gas transfer efficiency and allowing for larger dimensions for reduced shear. Such a concept may eventually benefit blood flow on the liquid side

ACKNOWLEDGMENTS

This work was supported in part by the NSF grant (ECCS-1951051).

REFERENCES

- [1] J. Feng, J. Yuan, and S. K. Cho, "Micropropulsion by an acoustic bubble for navigating microfluidic spaces," *Lab on a Chip*, vol. 15, no. 6, pp. 1554-1562, 2015.
- [2] J. Feng, J. Yuan, and S. K. Cho, "2-D steering and propelling of acoustic bubble-powered microswimmers," *Lab on a Chip*, vol. 16, no. 12, pp. 2317-2325, 2016.
- [3] F.-W. Liu and S. K. Cho, "3-D swimming microdrone powered by acoustic bubbles," *Lab on a Chip*, vol. 21, no. 2, pp. 355-364, 2021.
- [4] S. Sadhal, "Acoustofluidics 13: Analysis of acoustic streaming by perturbation methods," *Lab on a Chip*, vol. 12, no. 13, pp. 2292-2300, 2012.
- [5] M. Wiklund, R. Green, and M. Ohlin, "Acoustofluidics 14: Applications of acoustic streaming in microfluidic devices," *Lab on a Chip*, vol. 12, no. 14, pp. 2438-2451, 2012.
- [6] M. K. Tan, L. Yeo, and J. Friend, "Rapid fluid flow and mixing induced in microchannels using surface acoustic waves," *Europhysics Letters*, vol. 87, no. 4, p. 47003, 2009.
- [7] G. Destgeer, S. Im, B. H. Ha, J. H. Jung, M. A. Ansari, and H. J. Sung, "Adjustable, rapidly switching microfluidic gradient generation using focused travelling surface acoustic waves," *Applied Physics Letters*, vol. 104, no. 2, p. 023506, 2014.
- [8] J. Friend and L. Y. Yeo, "Microscale acoustofluidics: Microfluidics driven via acoustics and ultrasonics," *Reviews of Modern Physics*, vol. 83, no. 2, p. 647, 2011.
- [9] P. Tho, R. Manasseh, and A. Ooi, "Cavitation microstreaming patterns in single and multiple bubble systems," *Journal of Fluid Mechanics*, vol. 576, pp. 191-233, 2007.
- [10] P.-H. Huang *et al.*, "An acoustofluidic micromixer based on oscillating sidewall sharpedges," *Lab on a Chip*, vol. 13, no. 19, pp. 3847-3852, 2013.
- [11] J. A. Potkay, "The promise of microfluidic artificial lungs," *Lab on a Chip*, vol. 14, no. 21, pp. 4122-4138, 2014.

CONTACT

* S.K. Cho, tel: +1-412-624-9798; skcho@pitt.edu